Supernova simulation

project 2

Students names

Teresa Zorzi, Chiara Zerbinati,Matteo Sapori

July 25, 2022

Computational for physics and astrophysics

Contents

1 Physical background

The last moment of massive stars is marked by the ejection of their envelope through a powerful explosion that we call type II Supernovae. Such events are so energetic that they produce a shock in the surrounding environment, to the point that the entire ISM is blown away, leaving a so-called *Supernova remnant*, typically a neutron star or a black hole.

The typical energy output of a Type II SN is of the order of 10^{51} *erg*, which is the reference value that will be used in the simulation.

The purpose of this project is to simulate the consequences of a type II SN event.

Typically, SNs experience different phases that correspond to different evolutionary stages, namely:

- **Free expansion**. During which the surrounding ISM does not affect the velocity of expansion of the bubble of ejecta.

- **Sedov phase**. It is the most important phase. It begins just after the explosion and lasts up to 10^5 years. During this phase, the velocity of the shock front is supersonic but slowly decreasing.

- **Radiative phase**. In this phase, the shock front is almost steady and the luminosity is supported mainly by radiative recombination.

- **Quiescent phase, death**

For the purpose of this project, only the Sedov phase is considered.

2 Setting the problem

The code used to solve the problem is a modified and simplified version of the 'Zeus' code written in 1998 as a magneto-hydrodynamics simulator, adjusted to fit our necessity. In order to keep the computational difficulty as low as possible, the problem has been simplified as one-dimensional, making the points of the 1D grid correspond to the radii of the sphere at with we compute the solution step by step.

As in the first project, the grid is obtained as the sum of two decentralized grids (X_a and X_b) such that $X_a - X_b = 0.5 \cdot \Delta x$, to properly center the variables. The total lenght of the grid is set to 200 pc. We set the number of points in each grid to be 3000, thus making them separated by

$$\Delta x = X_a(i+1) - X_a(i) = X_b(i+1) - X_b(i) = 0.03 \ pc.$$

Points number 1 and 3000 are set as 'non-active points' and used to implement proper boundary conditions. Furthermore, point number 2 is set to be $x(2) = 0$, thus making it the first active point of the grid. Consequently, point number 1 corresponds to $x(1) = -\Delta x$. This is not a problem since this point is used only for the boundary conditions.

The original 'Zeus' program allows one to choose in which type of coordinates perform the calculations thanks to numerical scale factors; in this case, we have chosen to work in spherical coordinates.

2.1 Initial Conditions

After setting the grid, we proceeded by properly filling the initial conditions of the problem over the active points; the fourth one has been chosen as the radius of the volume that shall act as our supernova at $t = 0$. Thus, the value of energy density, pressure and temperature at these points and time can be computed as follows:

$$e(2) = e(3) = \frac{3 \cdot E_0}{4\pi \cdot X_a(4)^3}$$

$$p(2) = p(3) = (\gamma - 1) \cdot e(2)$$

$$T(2) = T(3) = \frac{e(2)}{c_v \cdot d_0}$$

Where $\gamma = 5/3$ is the gas constant. For the remaining points, we set the following initial conditions:

- v(i) = 0

- d(i) = $d_0 = 2 \cdot 10^{-24}$ gm cm^{-3}

- T(i) = $T_0 = 1 \cdot 10^4$ K

It's important to point out that the Supernova's energy output is injected before the time cycle begins.

3 The code

Our code simulates the Supernova explosion up to 10^5 years and takes snapshots at different times: in particular, we gather results at $2.10^4, 4.10^4, 6.10^4, 8.10^4$, and 1.10^5 years. This is done by implementing a main DO-loop containing the one that solves the hydrodynamics equations. Inside these loops, different variables (each of them named as a different monkey type) control the time flow: the first time steps have been taken shorter than the following ones in order to better simulate the first moments of the Supernovae. The code allows, if necessary, to print on the terminal every N (again, the value of N is controlled by a variable) time steps the values of quantities such as the number of cycles, the time, and the time step ($\Delta time$): this allows a real-time check of the simulation.

3.1 Stability condition

In order for the code to be stable, preventing the propagation and amplification of errors (in this case to avoid short-wavelength oscillations), the time steps must be small enough to satisfy the CFL(Courant-Friedrichs-

Lewy) stability condition.

Physically we can understand this condition as limiting the distance that a fluid particle can travel in one time step to be smaller than one grid zone.

This is represented by the equation:

$$\Delta t = \frac{C \cdot \Delta x}{v + v_s} \tag{1}$$

Where v is the fluid velocity and v_s is the speed of sound for the fluid itself.

In addition to that for the first time steps, the value of C is set to 0.01 and is incremented by 10% at each step up to 0.5.

3.2   The equations of hydrodynamics

The Supernova is simulated by solving the equations of hydrodynamics. Those are a set of hyperbolic partial differential equations. Two main formalisms can be used when solving those equations: Lagrangian or Eulerian. For the first, the frame reference is solid with the fluid particle [1], while in the Eulerian formalism, the frame is fixed. This is the main part of the code and it's divided into two main 'big' steps: the **source step** and the **transport step**.

	Lagrangian	**Eulerian**
conservation of mass	$\dfrac{D\rho}{Dt} + \rho \nabla \cdot v = 0$	$\dfrac{\partial \rho}{\partial t} + \nabla \cdot (v\rho) = 0$
conservation of momentum	$\rho \dfrac{Dv}{Dt} = -\nabla p$	$\dfrac{\partial v}{\partial t} + (v \cdot \nabla)v = -\dfrac{\nabla p}{\rho}$
conservation of energy	$\rho \dfrac{D}{Dt} \cdot \dfrac{e}{\rho} = -p\nabla \cdot v$	$\dfrac{\partial e}{\partial t} + \nabla \cdot (ev) = -p\nabla \cdot v$

where $\frac{D}{Dt}$ denotes the Lagrangian or comoving derivative:

$$\frac{D}{Dt} = \frac{\delta}{\delta t} + v \cdot \nabla \tag{2}$$

They are resolved using the method of finite differences with a time-explicit procedure. This method evaluates each part of the solution successively by updating the previous values.

For reference; we can write the dynamical equations schematically as:

$$\frac{\partial x}{\partial t} = S(x) \tag{3}$$

---

[1]In hydrodynamics a fluid particle is a volume element that contains enough particles to be statistically relevant, but enough small to non be comparable with the scale-dimension of the problem

If the operator $S(x)$ can be split in different parts, $S(x) = S_1(x) + S_2(x) + ...$ then finite differences method can be applied:

$$(x(t = t_1) - x(t = t_0))/\Delta t = S_1(x(t = t_0))$$
$$(x(t = t_2) - x(t = t_1))/\Delta t = S_2(x(t = t_1))$$
$$(x(t = t_3) - x(t = t_2))/\Delta t = ...$$

3.3 Covariance formalism

Inside the code is possible to perform computation in cartesian and spherical coordinates. To do so is necessary to introduce some *metric scale factors*. Here we will report only the factor for the spherical coordinates for the simple 1D scenario.

metric scale factors			
geometry	x1	g2	g31
Cartesian	1	1	1
Spherical	r	r	r

metric coefficients derivatives and volume			
geometry	$\partial g2/\partial x1$	$\partial g31 \partial x1$	dvl1
Cartesian	0	0	Δx
Spherical	1	1	$\Delta(r^3)/3$

3.4 Source Step

In the source step we solve finite-difference approximation to the differential equations:

$$\rho \frac{\partial v}{\partial t} = -\nabla p - p \nabla \Phi - \nabla \cdot q \tag{4}$$

$$\frac{\partial e}{\partial t} = -p \nabla v - q \nabla p \tag{5}$$

Where q is the *artificial viscosity*. Unlike the original ZEUS code, our does not contain a Poisson solver for the gravitational potential, so the term $\nabla \Phi$ is set to be equal to 0.

This step is all about updating the variables, no advection takes place. For this reason, a centered derivatives scheme is used in the source step.

NB: by this moment the superscript n denotes quantities at the n'th time step, while $n + 1$ (and so on) indicate subsequent steps. This part itself is divided into three substeps.

Substep I

Here we update the velocities accounting for the pressure gradients.
The finite differences equation solved in this step is:

$$\frac{v_i^{n+1} - v_i^n}{\Delta t} = -2\frac{p_i^n - p_{i-1}^n}{dxb_i(d_i^n + d_{i-1}^n)} \tag{6}$$

Note that: the pressure p_i^n is computed before this step using the equation of state in the approximation of perfect gas conditions so that $p_i^n = (\gamma - 1)e_i^n$.

Substep II

In this part of the code, we introduce the *artificial viscosity* (q); similarly to a real viscosity, the artificial viscosity acts by smoothing the flow near sharp gradients.
This term is added to the pressure in the hydro equation, thus $P \to P + q$ It's define as follows:

$$q = \begin{cases} C_2 d_i(v_{i+1} - v_i)^2, & \text{if } v_{i+1} - v_i < 0 \\ 0, & \text{if } v_{i+1} - v_i > 0 \end{cases} \tag{7}$$

Where $C_2 = l/\Delta x \approx 3$ is a dimensionless parameter that measures the number of zones over which the artificial viscosity will spread the shock.

We can better understand the role of artificial viscosity by writing the numerical Reynold number for the characteristic lengthscale λ :

$$R = \frac{Lv}{\nu} = \frac{(\lambda/\Delta x \Delta v_\lambda)}{q^2 \Delta v} \tag{8}$$

Where Δv_λ is the characteristic velocity variation on scale λ When R is large viscosity is not important over scales $\approx \lambda$ and the flow is smooth.

Using the artificial viscosity we then update both the velocity and the energy as follows:

$$\frac{v_i^{n+2} - v_i^{n+1}}{\Delta t} = -2\frac{q_i - p_{i-1}}{dxb_i(d_i^n + d_{i-1}^n)} \tag{9}$$

$$\frac{e_i^{n+2} - e_i^n}{\Delta t} = -q_i\frac{v_{i+1} - v_i}{dxa_i} \tag{10}$$

Substep III

Here we add the compression heating term (represented by the divergence of v) and solve the equation of conservation of energy:

$$e_{i,j}^{n+3} = [\frac{1 - (\Delta t/2)(\gamma - 1)(\nabla \cdot v)}{1 + (\Delta t/2)(\gamma - 1)(\nabla \cdot v)}] \cdot e_{i,j}^{n+2} \tag{11}$$

At the end of substep III is inserted the part of the code in which the radiative cooling is considered. Firstly the energy is updated by introducing the *cooling function* ($\Lambda(T)$):

$$\frac{e^{n+2} - e^n}{\Delta t} = -(\frac{d_i}{2.17 \cdot 10^{-24}})^2 \Lambda(T) \tag{12}$$

Then the temperature is recalculated over the whole grid using the new energy values, with the condition that the temperature is not allowed to be less than T for unperturbed ISM. By introducing this constraint we need to calculate again the energy associated with these new temperature conditions.

3.5 Transport Step

Now we take into account the fluid advection, for this reason an upwind scheme is used to solve finite difference approximations to the integral equations:

$$\frac{d}{dt} \int_V \rho dV = -\int_s \rho(v - v_s) \cdot dS \tag{13}$$

$$\frac{d}{dt} \int_V \rho v dV = -\int_s \rho v(v - v_s) \cdot dS \tag{14}$$

$$\frac{d}{dt} \int_V e dV = -\int_s e(v - v_s) \cdot dS \tag{15}$$

Where v_g in our case is zero and corresponds to the velocity for a moving grid.

These equations state that the rate of change of a quantity 'q' inside a volume (the so-called control volume) is equal to the divergence of the flux of q through the control volume surfaces. In the code we solve the following finite differences equations:

$$(q_i^{n+1}\tau_i^{n+1} - q_i^n \tau_i^n)/(\Delta t) = -(F_{i+1}^k - F_i^k)^{n+1/2} \tag{16}$$

The flux in the k'th direction is:

$$(F_i^k)^{n+1/2} = \langle (vk_{i,j} - vgk_i)q_{k,i}^\star A_{k,i} \rangle \tag{17}$$

Where $vk_i - vgk_i$ is the fluid velocity relative to the grid, $q_{k,i}^\star$ is the value of q interpolate to the interface of the control volume. The angle brackets denote that all quantities are time centered.

Given interpolated and time-centered values for a variable we can then proceed to construct time-centered fluxed and perform the advection.

$$F_i^1 = d_i^\star(v_i - vg1_i) \cdot g2a_i^{n+1/2} g3a_i^{n+1/2} dvl2a_i^n \tag{18}$$

where $d^\star$ is:

$$d^\star = \begin{cases} d_i, & \text{if} v_i < 0 \\ d_{i-1}, & \text{if } v_i > 0 \end{cases}$$

8

Thus the updated value for the flux is:

$$(F_{i+1}^1 - F_i^1) = -\Delta t(d_i^{n+1} A^{n+1} - d_i^n A^n) \qquad (19)$$

Where A denotes all the metric scale factors. Once the fluxes are calculated, advection for all the variables proceeds in the same way:

$$d_i^{n+1} = d_i^n - \frac{\Delta t}{\Delta X_a}(F_{i+1}^n - F_i^n) \qquad (20)$$

$$e_i^{n+1} = e_i^n - \frac{\Delta t}{\Delta X_a}(F2_{i+1}^n - F2_i^n) \qquad (21)$$

$$S_{i+\frac{1}{2}}^{n+1} = S_{i-\frac{1}{2}}^n - \frac{\Delta t}{\Delta X_b}(F3_{i+1}^n - F3_i^n) \qquad (22)$$

Here S is the momentum. Notice that it is centered at $i + \frac{1}{2}$.

3.6 Boundary conditions

Inside the code, the boundary conditions are implemented through a subroutine that is called for every time we need to impose our conditions. we choose to use *reflecting boundary conditions*, in with the value of the variables in the non active points are set equal to the corresponding values of their images among the active points, more precisely:

$$value(i_{max}) = value(i_{max} - 1)$$
$$value(1) = value(2)$$

4 Preliminary results, cartesian shock tube

Once the code is complete, we can design a problem that tests all transport and source terms. For 1D hydrodynamics, the most used test of this kind is the *shock tube test*. It involves setting up two discontinuities: a hot dense gas on the left, and a cold rarefied gas on the right and letting them interact.
A problem of this kind is called a *Riemann problem*, for with the solution is known and can be compared with the numerical results [fig 10]
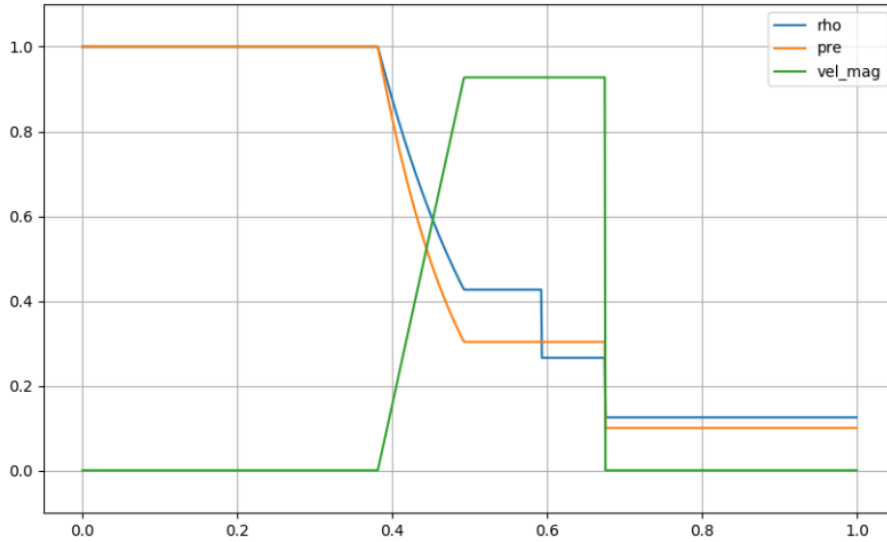
Figure 1: Shock tube analitical results

Note: the test is performed in cartesian coordinates.
Results for this preliminary test are here reported and can be verified to be consistent with the analytical solution.
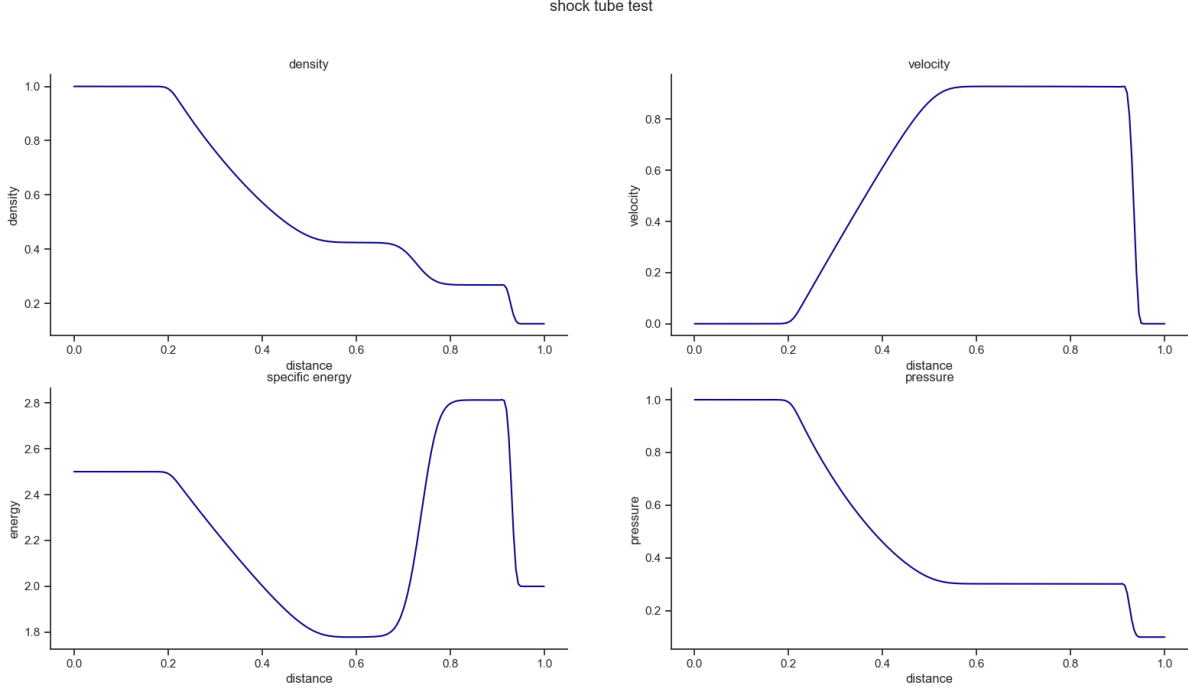
Figure 2: Shock tube results for a grid of 100 points

5 Main results

We run the code at different times for different cooling and environmental conditions; more precisely, for the standard ISM case, we investigated the impact of cooling through radiation by running the code with and without the effects operated by the cooling function ($\Lambda(T)$). The entire 'cooling phase' can be skipped by changing the value of the corresponding control variable (namely 'no$_c$$ooling'$).

Furthermore, we also checked the results for the case of Hot Ionised Medium (HIM) and Cold Ionised Medium (CIM).

5.1 standard ISM without cooling

For the case of standard ISM we used the following values for density and temperature:

- **Density** $\rightarrow$ d=10^{-24} $g.cm^{-3}$

- **Temperature** $\rightarrow$ T=10^4 K

When the effects of the cooling function are neglected, we expect an almost perfect agreement with the *Sedov*

Solution since it corresponds to an adiabatic case [figure 6].

The evolution of the simulation follows the theoretical model described by the Sedov solution.

Is also possible to notice that the discontinuity is spread across multiple points instead of only one as defined by the model, this is due to the integration of the artificial viscosity.

In the graphs is evident the formation of the shock front; in particular, the max density is approximately 4 times the initial density, as predicted by the strong shock model.

Behind the shock a hot bubble is formed. This structure is pressure-supported and its temperature is very high. Without the cooling effect the shape of the shock does not change significantly over time (we will see that this is not the case when the cooling is considered).

By comparing the results at different times is possible to notice the weakening of the shock and the relative decrease of the velocity of the discontinuity, This is once again in line with the theoretical model and is due to the progressive decrease of the internal pressure of the bubble (clearly visible in the graph).

Figure 3: ISM conditions after the supernova. No cooling

5.2 Standard ISM with cooling

The cooling effects are operated trough the *cooling function*:
by definition, it's a function that relates the temperature and the density of a gas with the rate at which it cools.
The standard cooling function is computed for different chemical and physical compositions. For the project, we use an approximation in which the numerical density is not considered, the chemical composition either, and the only dependence is that of the temperature. Our function is defined as follows:
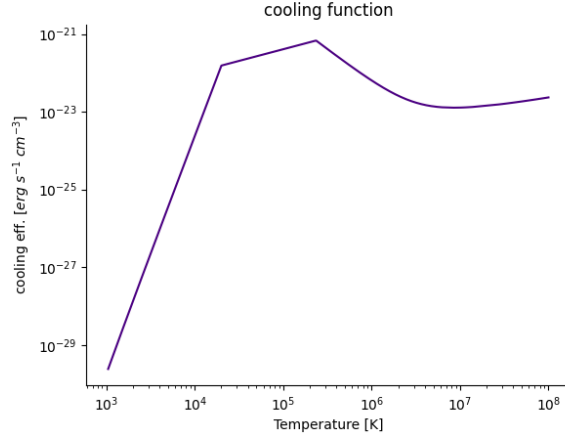

Figure 4: cooling function used in the project

$$T > 0.02 \text{ Kev} \longrightarrow \Lambda(T) = 10^{-22}(8.6 \cdot 10^{-3}T_{kev}^{-1.7} + 0.058T_{kev}^{0.5} + 0.063)$$

$$0.02 < T < 0.017 \text{ Kev} \longrightarrow \Lambda(T) = 6.72 \cdot 10^{-22}(\frac{T_{kev}}{0.02})^{0.6}$$

$$T < 0.017 \text{ Kev} \longrightarrow \Lambda(T) = 1.54 \cdot 10^{-22}(\frac{T_{kev}}{0.0017})^{6}$$

As before, the results are reported in figure 5.
By comparison with the previous results, is clear that the general behavior does not change much. This is not completely true for the shock front, whose shape mutates with time. Those are the effects of the cooling we are looking for: where the gas gets heated and compressed it also lose more energy via radiation, de facto slowing down the front and making the shell thinner.
The cooling effects are also noticeable in the hot bubble region. This part of the structure loose energy way faster than in the case of no cooling and so its pressure is lower (at fixed times) if compared with the simulation without cooling.
The pressure inside the hot bubble is again the main driver of the expansion, this time, however, is notable how the pressure gradient near the shock changes more drastically with time. We can see how, toward the end of the simulation, the pressure gradient becomes negative. This is another effect caused by the cooling and goes with an increase in radiative emissivity.
Another effect of this increase in radiative emission is that this time, the shock velocity does not decrease as rapidly as before but it settles down (more or less) at around 200 $km.s^{-1}$. This is desired since the velocity is proportional to $-dP$. The same behavior can be seen in the temperature profile; in line with what has been said before, it became basically constant.
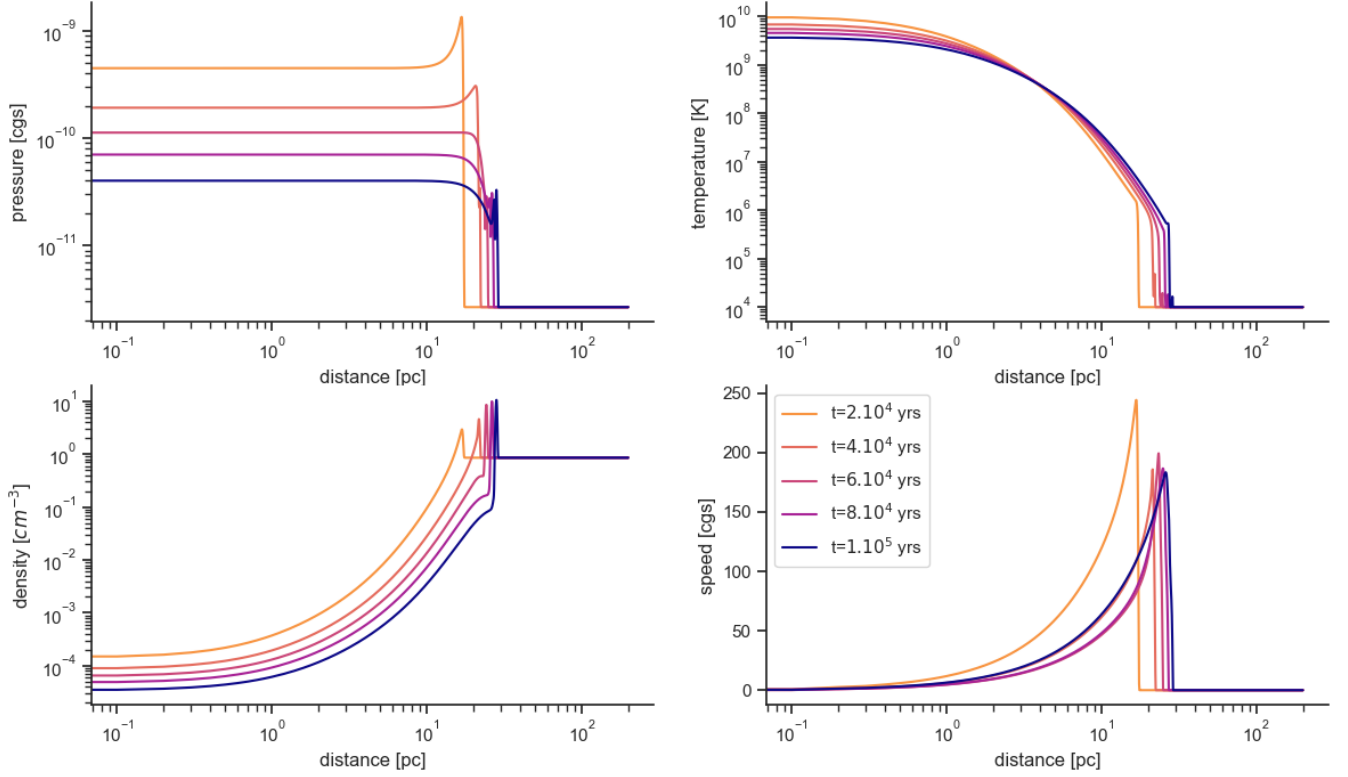
Figure 5: ISM condition after the supernova. With cooling

5.3   Shock radius and Sedov solution

Even in the most simple one-dimensional case, there are no real indications telling us where the shock wave is exactly. However, this is not a real problem since we have data about all the important physical parameters. In our case, the shock radius of the supernova has been taken as the value of the grid at which the velocity of the fluid is the highest. In the case of homogeneous ISM, this gives us the exact position of the shock, we will see that this approach is no more valid when the initial ISM is no more constant.

These values for the position of the shock front are then compared to the analytical approximation: the *Sedov solution* [eq 23]. Again, with and without cooling:

$$R_s(t) \approx 1.15 \cdot (\frac{E_{SN}}{d_0})^{1/5} t^{2/5} \tag{23}$$

As can be seen, when the cooling is neglected, our results are almost in perfect agreement with the Sedov solution. Instead, when the radiation cooling is considered, our solution starts to deviate from the analytical one after 40 000 years. This is when the radiative phase begins and the shock front starts to slow down.
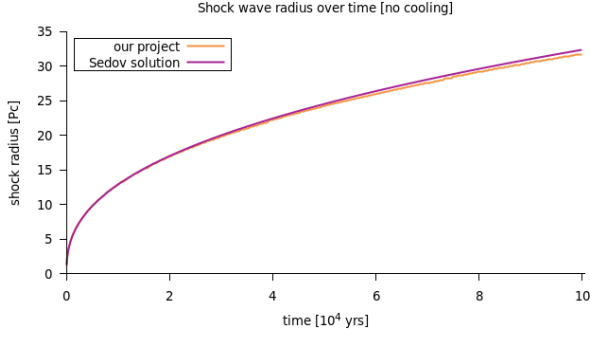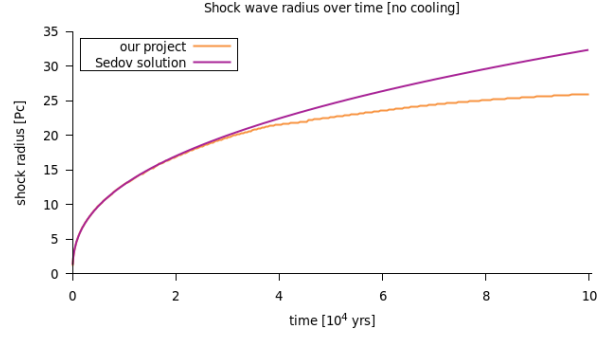
Figure 6: Sedov. No cooling

Figure 7: Sedov. With cooling

5.4   X-ray luminosity and Energy

The X-ray luminosity and the Energy output are computed at the end of each time step. No differential equations are solved in both cases.

The kinetic and thermal energies are integrated over the grid and then added together to obtain the total energy as follows:

$$E_{kin} = \sum_i \frac{1}{2} m(i) v(i)^2 \tag{24}$$

$$E_{th} = \sum_i \frac{4\pi}{3} (x(i+1)_a - x(i)_a)^3 e(i)_{th} \tag{25}$$

$$E_{tot} = E_{kin} + E_{tot}, \tag{26}$$

where 'i' indicates the i'th point of the grid.

Energy values are plotted with respect to time in Figure 8 and Figure 9.

Without the cooling effects all the energy is stored in the form of kinetic and thermal energy, thus our total energy, by conservation, should remain constant over time, With a mean value equal to 10^{51}; that corresponds to the original energy of the supernova.

However, by looking at fig 8, is clear that this is true only in a time-averaged sense: at the beginning, our total energy is in fact overestimated, while at the end is underestimated. This happens because our code is not completely conservative, and also because we decided to solve only first-order accurate FDE.

When the cooling is considered most of the losses are due to radiation cooling. In the beginning, energy losses are negligible and the behavior of the energies is the same as in the first scenario. After 40 000 years, the radiative phase reaches its maximum and the energy stars get irradiated away. The cooling transforms thermal energy into radiation.

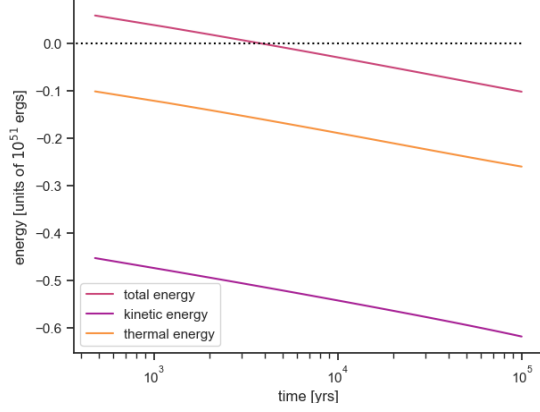The increase in kinetic energy is due to the change in pressure gradient as discussed before.

15

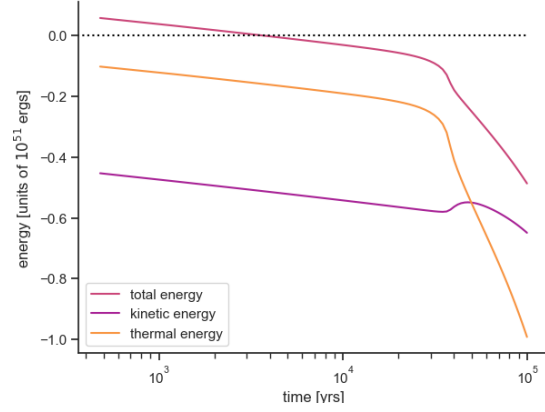*Figure 8: Energy output without cooling*

Figure 9: Energy output with cooling

X-ray luminosity is computed like the energies, as a sum over the grid. Only the plasma with a temperature larger than 10^6 K takes part in the emission.

$$L_x = \sum_i \frac{4\pi}{3}(x_a(i+1) - x_a(i))^3 n(i)^2 \cdot \Lambda(T(i)) \tag{27}$$

Where $\Lambda(T)$ is the cooling function.

Here the luminosity values are plotted. Again we compare results both in the case of radiation cooling and not. The results are in line with what we expected; when the cooling is considered, fewer points of the grid will have a temperature greater than 10^6 K, so the total luminosity should be less than in the case where the cooling is neglected. For the same reason, the difference becomes larger as time pass.

Figure 10

6   Different environmental conditions

Case of Hot Ionized Medium:

The Hot Ionized Medium (HIM) is one of the three main phases of the ISM. It is mainly composed of gas shock heated by supernovae or AGN activity with high temperature and low density.

This means that running the simulation in these conditions is almost like simulating the death of a massive star in the galactic bulge of our galaxy (though this is not a realistic scenario, SN II tends to explode in a more dense environment, where star formation is ongoing) or in a star-forming region that has already experienced supernovae explosions.

We want to investigate the behavior of the simulation by changing only the environmental parameters of temperature and density. The solution is computed in the same way as before and no other conditions are set.

We used the following initial conditions for density and temperature:

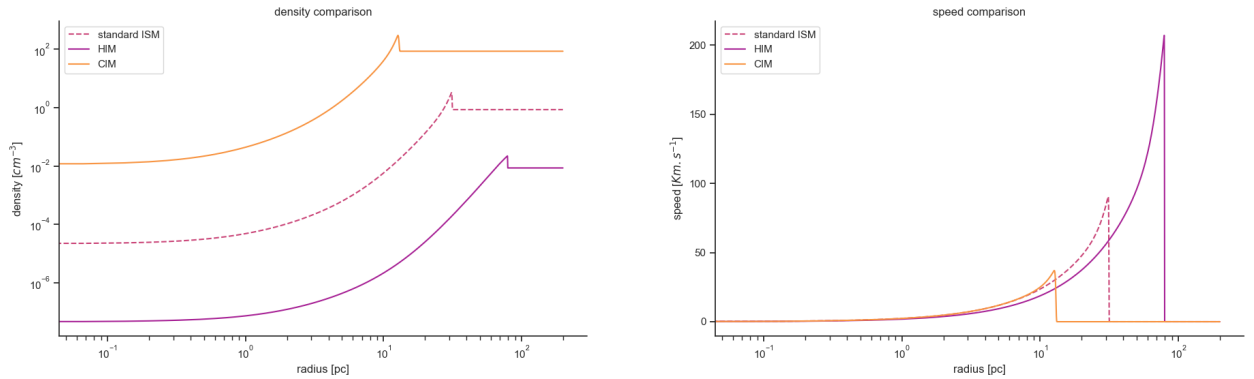- T $= 1 \cdot 10^6$ K

- d $= 2 \cdot 10^{-26}$ $g.cm^{-3}$

Case of cold ISM:

cold ISM is typical of star formation regions, where molecular hydrogen is the main component and high-energy photons of newly formed stars partially ionize the surrounding ISM. In this case we use those values for density and temperature:
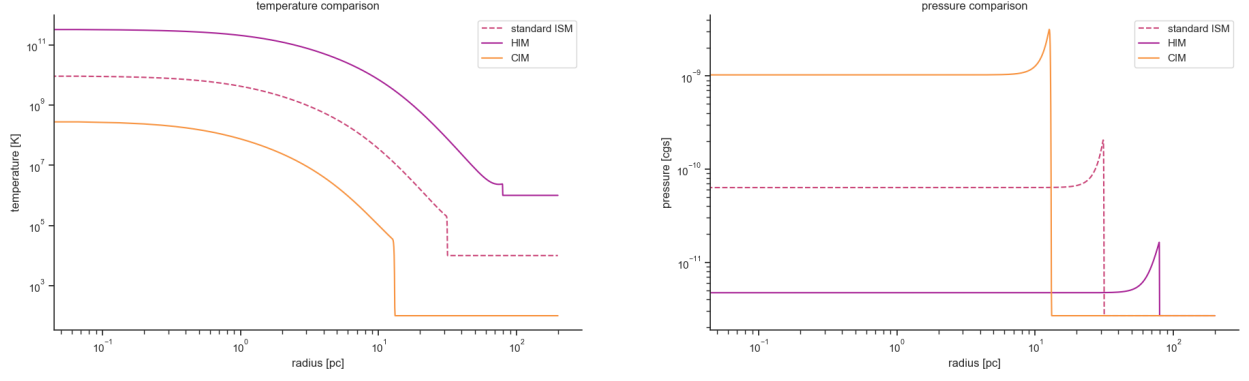
- T $= 1 \cdot 10^2$ K

- d $= 2 \cdot 10^{-22}$ $g.cm^{-3}$

The numerical results can be seen in the following figures:

Note; these results are obtained without considering the cooling effects, data from previous simulations (the ones with standard ISM) are the ones with dotted lines.

By looking at the graphs is possible to notice that the denser the environment get, the slower the shock wave became, as expected.

6.1 Sedov solution for different ISM conditions

This section is dedicated to the comparison of the results of our project with the Sedov solution for different density values when cooling is neglected.
Recalling the Sedov approximation:

$$R_s(t) \approx 1.15 \cdot (\frac{E_{SN}}{d_0})^{1/5} t^{2/5}$$

Is clearly visible that the radius of the supernova, for fixed times, should be larger for lower mean densities d_0,because the expansion velocity is greater.By looking at [figure 11] we can see that this is in fact the case.

Figure 11: Sedov approximation for different ISM condition

7 Stellar winds phase

Up to now, we considered a homogeneous ISM. This is just an educated guess of the real conditions. A more realistic simulation would take into account also how the star shapes the environment during her life span. To do so, we investigate the effects of the stellar winds phase that precedes the supernova, and then the outcome is used as the initial conditions for the simulation.

To properly simulate this phase the code has been slightly modified: like for the cooling effects, the S.W. phase is regulated by the value of a boolean control variable, namely '*winds*'.

If the condition 'winds == True' is satisfied, then the simulation proceeds as follows:

I) The max duration of the simulation is set to one million years.

II) The hydrodynamics solver calculates the time steps and solves the simulation with a constant injection of matter and energy by the star, constant initial velocity, and temperature of the winds.

III) as soon as the stellar winds phase terminates the variable winds is set to False and the grid values for p, T,d, and v are set as initial conditions [figure 12,13] for the supernova.

The code then proceeds to simulate the supernova just like before.

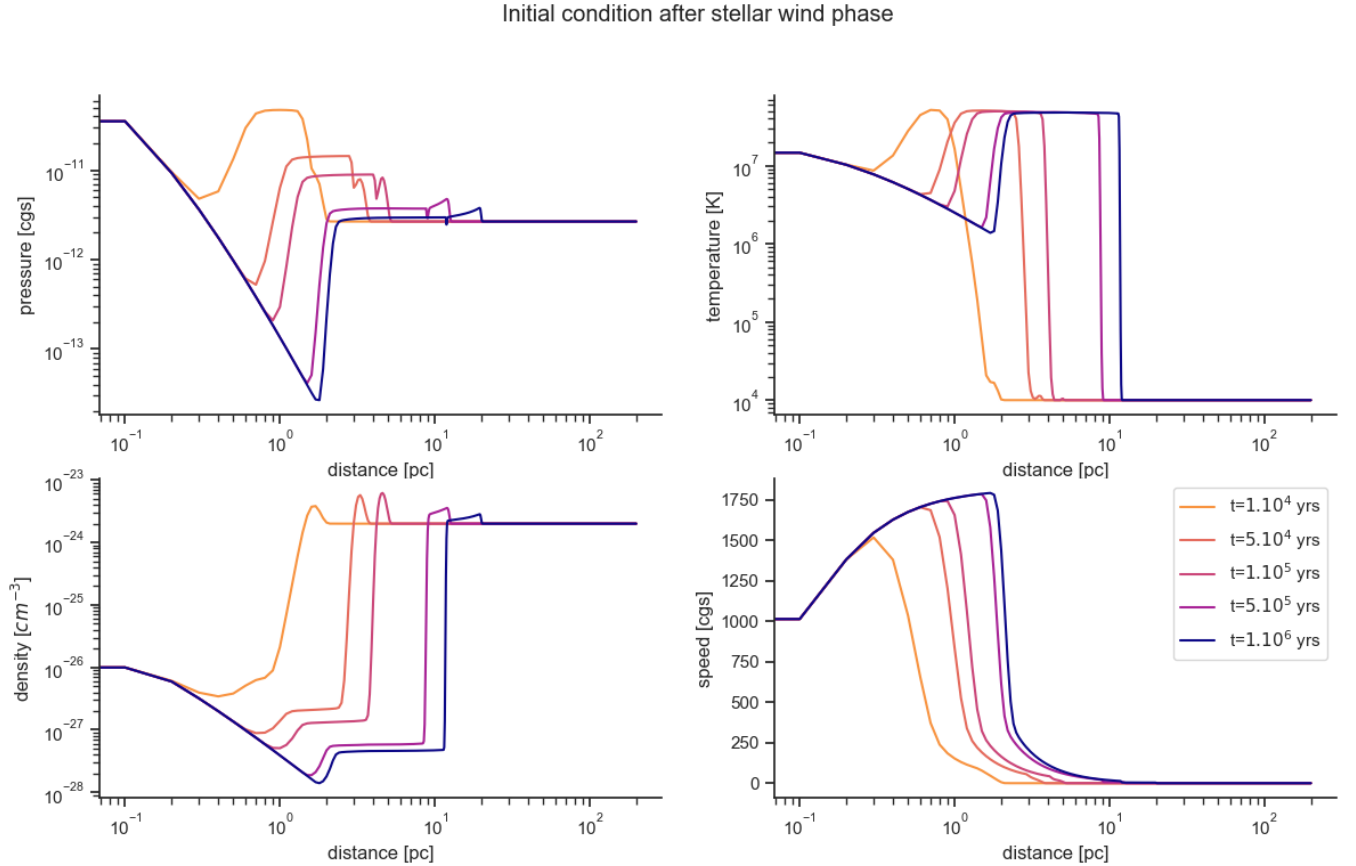Again, results are presented with and without the cooling effects.

Figure 12: *Initial conditions before the supernova if stellar winds and cooling are considered.*
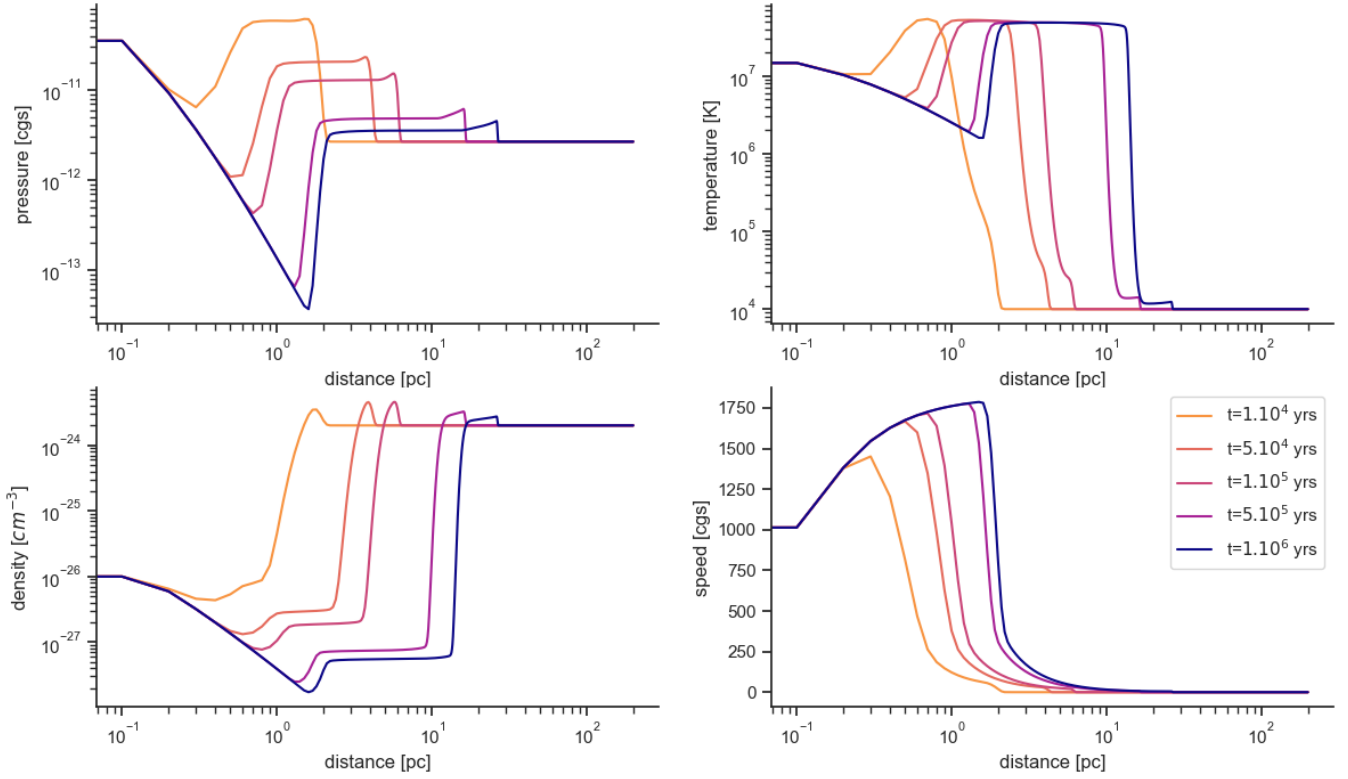
Figure 13: Initial conditions before the supernova if stellar winds are considered. NO cooling

7.1 Stellar wind bubble

Massive stars usually produce very strong stellar wind during their lifespan. This stellar wind interacts with the initial ISM and forms two shocks: a forward shock, that propagates into the ISM, and a reverse shock that propagates back into the stellar wind. The surrounding environment gets broken into four regions [figure 12,13, density plot]:

I)The unshocked stellar wind
II)The shocked stellar wind
III) The shocked ISM
IV)The unshocked ISM.

Inside region I the number density is given by:

$$\rho_I = \frac{M'}{4\pi m_p v_w r^2} \sim r^{-2} \tag{28}$$

where M' is the mass loss rate, v_w is the wind velocity, and r is the radial distance.
The bubble increase in size until the swept-up is comparable with the mass of the wind, this is where region

II began. In this region, a hot bubble is formed, here density, pressure, and temperature are almost constant.

$$T_{II} \approx \frac{3\mu m_p v_w^2}{16K}$$

$$p_{II} \approx \rho_I v_w^2$$

Region III is a thin, dense shell, containing most of the swept-up ISM, here the density is approx 4 times the density of the initial ISM.

For our project, we choose a mass loss rate of 10^{-5} solar masses per year, and a wind initial velocity of 1000 $km.s^{-1}$.

The injection, like for the supernova, takes place in the first 3 active points of the grid; but this time is continuum, and new energy and matter are injected at each time cycle.

In the case of stellar winds the new energy is represented by the mechanical luminosity [eq 29] of the wind since it is by far greater than the associated thermal energy.

$$L_{mec} = \frac{1}{2} M_{lost}.\Delta t.v_w^2 \tag{29}$$

In our case, the energy injected per year by our star is of the order of 10^{43} erg. Thus, after 1.000.000 years, the total energy injected in the ISM should be of the order of 10^{49-50} erg. A value almost in line with very massive stars, for which the total energy of their winds during their life span could easily be of the order of 10^{51} or even greater.

7.2   Results

Results for the supernova simulation are plotted in [figure **??**] and without cooling [figure **??**]. Some common features are still present, like the hot gas bubble and the visible shock front.

In both cases (cooling and not cooling), the max value for the velocity of expansion, is lower this time. This happens because, after the free expansion phase, the supernova shock front impacts the density barrier generated by the wind's shock (this is visible in the behavior of the kinetic energy graph [fig 16,17]). This time is not possible to identify the shock radius as the point with the maximum velocity, not even density or pressure. We instead used the point with the greater viscous term (represented by the artificial viscosity). Still, the results are not perfect, but they converge to the Sedov solution. Looking at the energy graph with cooling, this time the energy starts to get irradiated away from the first moment. This happens because of the nonhomogeneous ISM, with zones at high temperatures from the beginning.

Important note: Temperature profiles are not correct; for temperatures greater than 10^{10} K the concept itself of temperature is no more physically useful since such high energies are associated with relativistic regimes. Our cooling function does not account for such conditions, for this reason, take this result with a grain of salt.
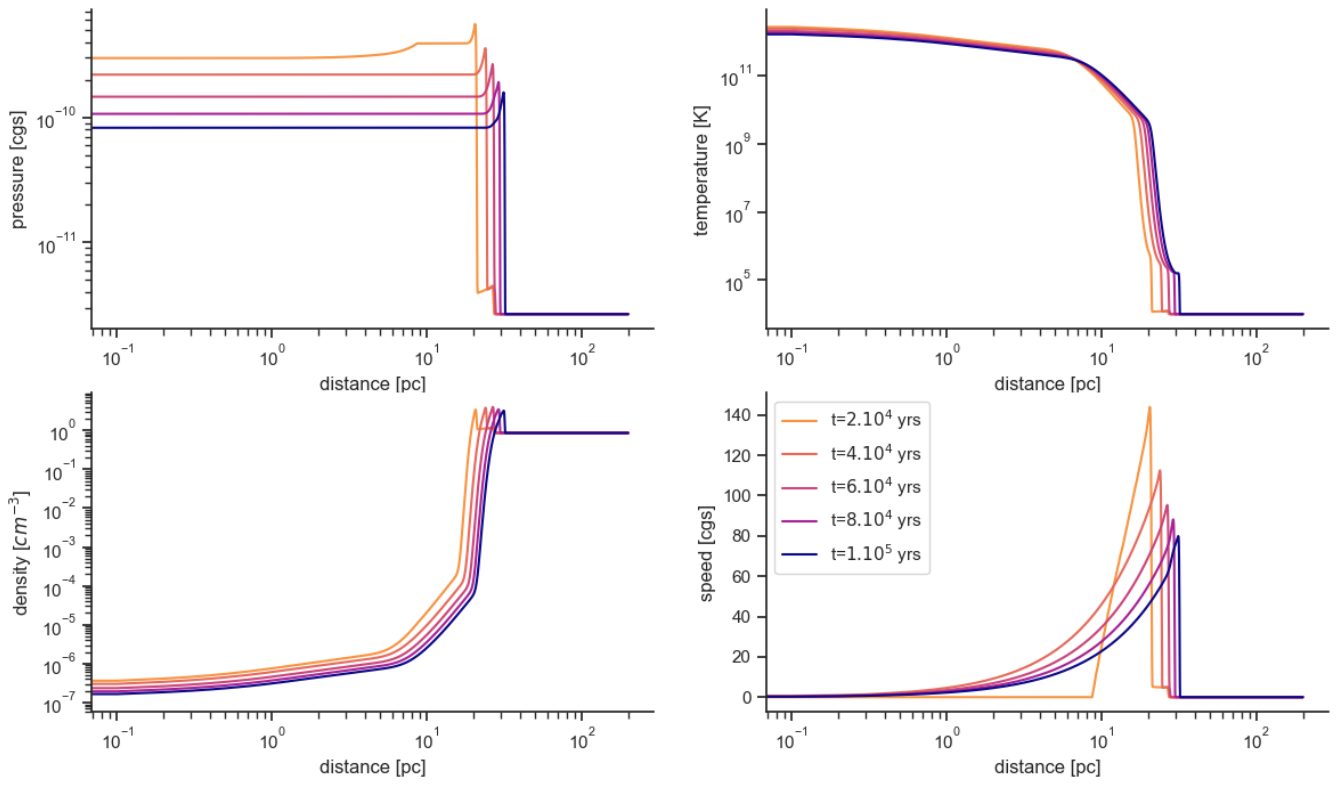
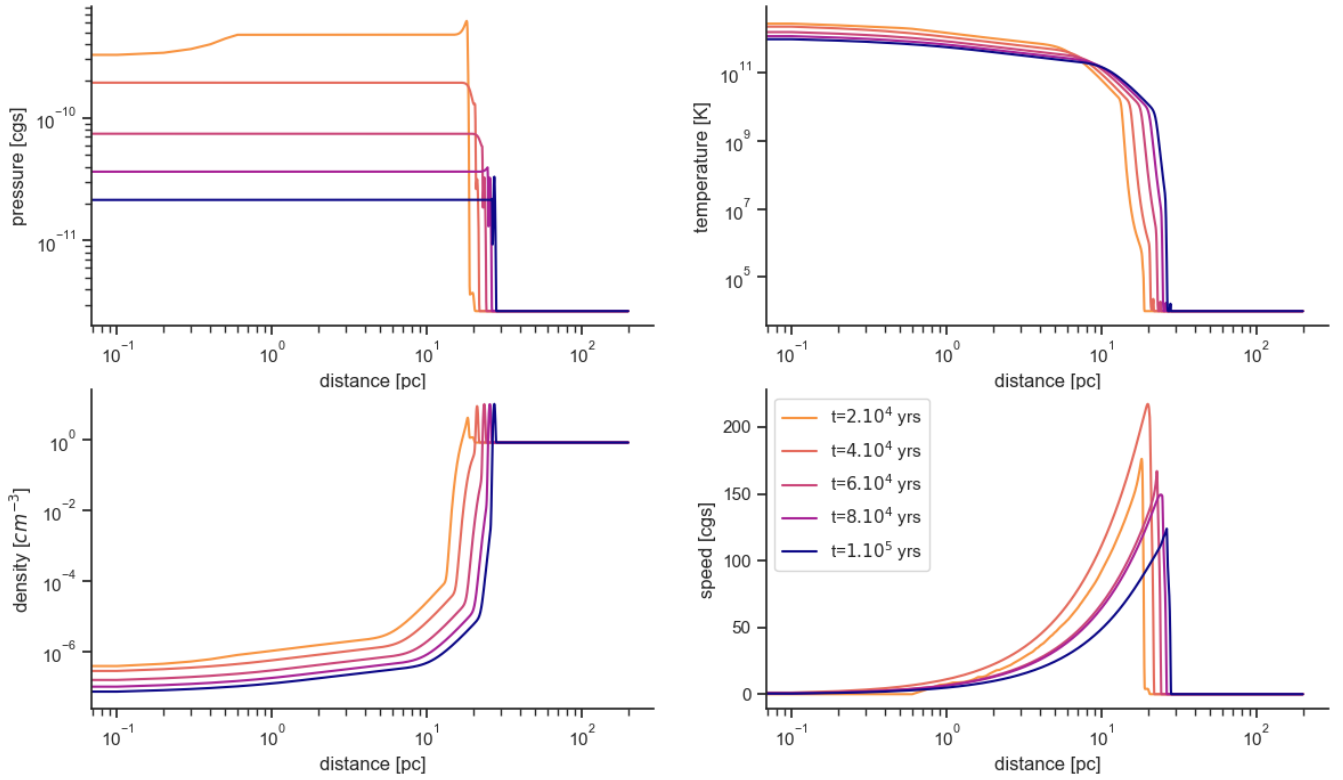*Figure 14: ISM condition at the end of the simulation. No cooling*

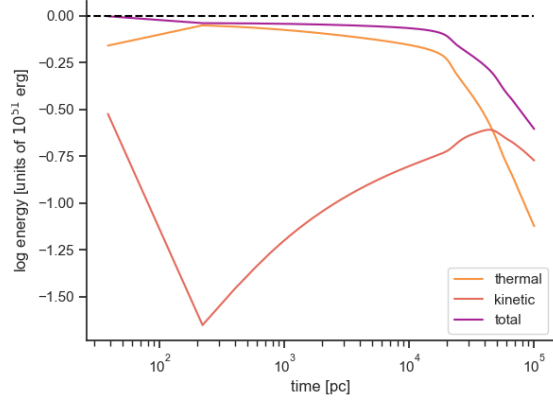*Figure 15: ISM condition at the end of the simulation. With coolin*
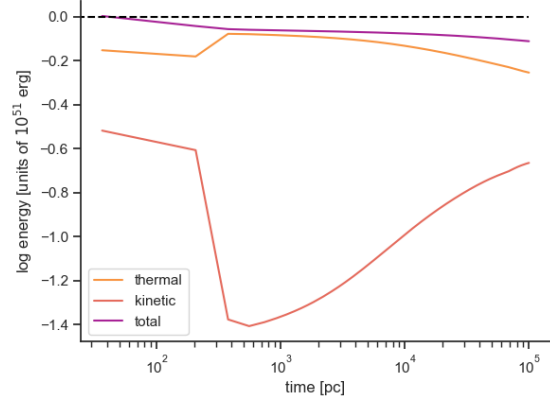
Figure 16: Energy output with cooling
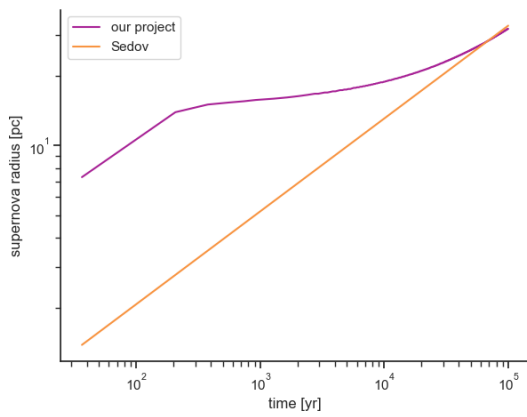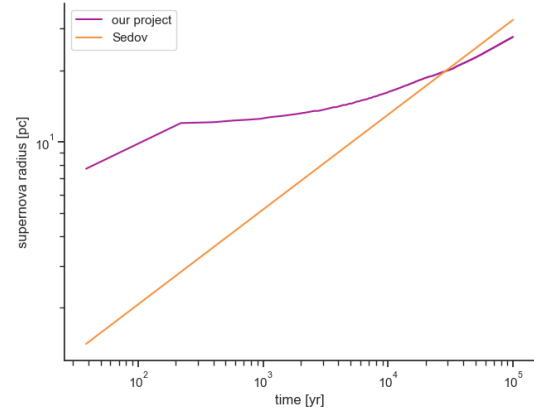

Figure 17: Energy output without cooling

Figure 18: Sedov. No cooling

Figure 19: Sedov. With cooling

23